Received: 3 September 2019 | Revised: 2 December 2019 | Accepted: 28 December 2019

DOI: 10.1002/ddr.21639

RESEARCH ARTICLE

DDR WILEY

Novel 3-aryl-5-substituted-coumarin analogues: Synthesis and bioactivity profile

Eleni Kavetsou[1] | Annita Katopodi[1,2] | Letta Argyri[2] | Eirini Chainoglou[3] | Eleni Pontiki[3] | Dimitra Hadjipavlou-Litina[3] | Angeliki Chroni[2] | Anastasia Detsi[1]

[1]Laboratory of Organic Chemistry, School of Chemical Engineering, National Technical University of Athens, Athens, Greece

[2]Institute of Biosciences and Applications, National Centre for Scientific Research "Demokritos", Athens, Greece

[3]Laboratory of Pharmaceutical Chemistry, Faculty of Health Sciences, School of Pharmacy, Aristotle University of Thessaloniki, Thessaloniki, Greece

Correspondence
Anastasia Detsi, Laboratory of Organic Chemistry, School of Chemical Engineering, National Technical University of Athens, Heroon Polytechniou 9, Zografou Campus, Athens 15773, Greece.
Email: adetsi@chemeng.ntua.gr

Funding information
European Regional Development Fund; European Social Fund; State Scholarships Foundation

Abstract

Eighteen 3-aryl-5-substituted-coumarins—six 5-acetyloxy-derivatives, six 5-hydroxy-derivatives, and six 5-geranyloxy-derivatives—were synthesized, structurally characterized and their antioxidant activity, lipoxygenase inhibitory ability, as well as their cytotoxic activity against human neuroblastoma SK-N-SH and HeLa adenocarcinoma cell lines were evaluated. The 5-acetyloxy-compounds **3a-3f** were found to be the best cytotoxic agents among all the compounds studied. The bromo-substituted coumarins **3a** and **3b** were remarkably active against HeLa cell line showing IC_{50} 1.8 and 6.1 μM, respectively. Coumarin **5e** possessing a geranyloxy-chain on position 5 of the coumarin scaffold presented dual bioactivity, while 5-geranyloxy-coumarin **5f** was the most competent soybean lipoxygenase inhibitor of this series (IC_{50} 10 μM). As shown by in silico docking studies, the studied molecules present allosteric interactions with soybean lipoxygenases.

KEYWORDS

acetyloxy-moiety, coumarins, cytotoxicity, lipoxygenase, molecular modeling, oxyprenylated analogues

1 | INTRODUCTION

Coumarins are naturally plant-derived or synthetically obtained substances that belong to the benzopyrone family (Detsi, Kontogiorgis, & Hadjipavlou-Litina, 2017). The wide bioactivity array, such as antioxidant (Matos et al., 2017), anti-inflammatory (Melagraki et al., 2009; Roussaki et al., 2014), anticancer (Kavetsou et al., 2017; Ricci et al., 2018), antivirus (Atta-ur-Rahman., 2018), and neuroprotective (Okuyama et al., 2013), renders coumarins attractive for further evaluation as novel therapeutic agents. Research has shown that substitution on the coumarin scaffold strongly influences its pharmacological profile. Thus, the structural modification of the coumarin core in the pursuit of biologically active multi-targeting compounds is a constantly intriguing research item (Garazd, Garazd, & Lesyk, 2017).

Oxyprenylated compounds (isopentenyloxy, geranyloxy, farnesyloxy compounds, and their biosynthetic derivatives) have attracted the scientific interest only in the last decade, while for years, they were considered just as biosynthetic intermediates of C-prenylated products (Alhassan, Abdullahi, Uba, & Umar, 2014). Therefore, their biological activities have recently started to be explored. Fiorito and coworkers (Fiorito, Epifano, Taddeo, & Genovese, 2018) presented in 2018 the key role of coumarins bearing a prenyloxy moiety, in the modulation of melanogenesis using murine Melan-a cell line (Fiorito et al., 2018). They have also reported the ability of plant isolated prenyloxy coumarins to inhibit RAW 264.7 proliferation (Genovese et al., 2017). Moreover, it has lately been demonstrated that oxyprenylated coumarins were strong inhibitors of different types of lipoxygenases (e.g., 5-LOX and 15-LOX) (Fiorito, Epifano, Preziuso, et al., 2018; Kavetsou et al., 2017).

Lipoxygenases (LOX) are iron-containing enzymes that catalyze the oxidation of polyunsaturated fatty acids such as linoleic acid (in plants) and arachidonic acid (in mammals) at specific positions to hydroperoxides (Detsi, Majdalani, Kontogiorgis, Hadjipavlou-Litina, & Kefalas, 2009; Simijonović et al., 2018). Inhibitors of LOX had initially

attracted attention as potential agents for the treatment of inflammatory and allergic diseases. However, the association between chronic and persistent inflammation and the development of malignant diseases through certain pathways has now expanded their therapeutic potential (Crusz & Balkwill, 2015; Genovese et al., 2017; Schneider & Pozzi, 2011).

Oxidative stress has been associated with the inflammation process. Reactive oxygen species are produced during the inflammation process by phagocytic leukocytes that invade the tissue. Moreover, these reactive species are involved in the cyclooxygenase (COX)- and lipoxygenase (LOX)-mediated conversion of arachidonic acid into proinflammatory intermediates. The implications of COXs and LOXs have been discussed in numerous types of cancers, including colon, pancreas, breast, lung, skin, urinary bladder, liver, and so on (Orafaie, Matin, & Sadeghian, 2018).

Although much research has been conducted and significant progress has been reported, cancer is still the second major cause of death globally. It is noteworthy that current chemotherapeutic agents present low effectiveness due to the development of multidrug resistant cancers, while they display severe side effects (Bian et al., 2018; Mansoori, Mohammadi, Davudian, Shirjang, & Baradaran, 2017; Senapati, Mahanta, Kumar, & Maiti, 2018). Therefore, target identification and searching for new anticancer drugs endowed with cytotoxic activity is of great importance, while plant-derived heterocyclic compounds and their derivatives have always consisted an invaluable source for the discovery of new therapeutic agents (Bathula et al., 2015; Demir, Özen, Ünlüsoy, Öztürk, & Bozdağ-Dündar, 2019; Hati et al., 2016). Interestingly, heterocyclic scaffolds such as coumarins have a tremendous ability to regulate diverse range of cellular pathways, thus they can be regarded as key structures for multi-targeting purposes (Thakur, Singla, & Jaitak, 2015). Specifically, coumarins' anti-tumor responses are related to various mechanisms such as apoptosis induction, inhibition of cell growth, and of DNA-associated enzymes, as topoisomerase (Majumdar et al., 2015). Characteristic examples of natural coumarins possessing anticancer effects are auraptene (Hasan, Genovese, Fiorito, Epifano, & Witt-Enderby, 2017; Lee et al., 2017), umbelliprenin (Kavetsou et al., 2017), and umbelliferone (Mazimba, 2017).

Herein, in continuation to our previous studies (Kavetsou et al., 2017), we present the synthesis, structural characterization, and in vitro biological evaluation of 18 multi-substituted coumarin analogues. The aim of the current research was to design and synthesize novel coumarin derivatives with multi-targeting effects against both inflammation and cancer cell viability based on our previous work. Antioxidant activity, soybean LOX inhibitory activity, as well as cytotoxicity of the novel derivatives against human neuroblastoma cell line SK-N-SH and cervical cancer cell line HeLa were determined.

In addition, in silico docking studies were performed in soybean LOX and provided useful interpretation of the experimental results whereas the drug-likeness of the derivatives was determined from the theoretical calculation of various molecular properties.

2 | MATERIALS AND METHODS

2.1 | Chemicals and instruments

The chemicals used for synthesis, analysis, and evaluation were purchased from Sigma-Aldrich and used without further purification. NMR spectra were recorded on Varian 300 & 600 MHz spectrometer and the HR-MS spectra on a UHPLC-MSn Orbitrap Velos-Thermo mass spectrometer at the National Hellenic Research Foundation. Melting points were obtained using a Gallenkamp MFB-595 melting point apparatus and are uncorrected. Lipophilicity values were calculated in silico.

2.2 | Inhibition of linoleic acid lipid peroxidation

The assay was performed according to the experimental procedure from our previous publications (Melagraki et al., 2009; Roussaki et al., 2014; Roussaki, Kontogiorgis, Hadjipavlou-Litina, Hamilakis, & Detsi, 2010). In an aqueous solution spectrophotometrically at 234 nm was monitored and recorded the production of conjugated diene hydro peroxide by oxidation of sodium linoleate. Ten microliters of the 16 mM sodium linoleate solution was added to the UV cuvette containing 930 μL of 0.05 M phosphate buffer, pH 7.4 prethermostated at 37°C, under air by the addition of 50 μL of 40 mM AAPH solution which was used as a free radical initiator. Ten microliters of the appropriate solutions of the tested compounds were added in the mixture, whereas the same level of Dimethylsulfoxide (DMSO) was used as a blanc for the measurement of lipid oxidation. The rate of oxidation at 37°C was monitored by recording the increase in absorption at 234 nm caused by conjugated diene hydro peroxides. The results were compared with the appropriate standard inhibitor Trolox (93%).

2.3 | Soybean LOX inhibition study in vitro

The assay was performed according to the experimental procedure from our previous publications (Melagraki et al., 2009; Roussaki et al., 2010; Roussaki et al., 2014). The tested compounds as stock solutions were dissolved in DMSO. Ten microliters were incubated at room temperature with sodium linoleate (100 mM) and 0.2 ml of enzyme solution ($1/9 \times 10^{-4}$ *w/v* in saline) in buffer pH 9 (tris) at room temperature (final volume 1 ml). The conversion of sodium linoleate to 13-hydroperoxylinoleic acid at 234 nm was recorded. The results were compared with the appropriate standard inhibitor Nordihydroguaeretic acid NDGA (IC_{50} 0.45 μM). Several concentrations were used for the determination of IC_{50} values. The results are given expressed as IC_{50} values.

Experiments were repeated four times (experimental replicates). The results were expressed as mean ± *SD*. Statistical comparisons were made using the Kruskal Wallis test. Statistically significant difference was defined as $p < .05$.

2.4 | Cell culture

Human neuroblastoma SK-N-SH cells (ATCC) were cultured in Minimal Essential Medium (MEM) Earle's supplemented with 2 mM L-glutamine, 0.1 mM nonessential amino acids, 1 mM sodium pyruvate, 1.5 g/L sodium bicarbonate, 10% Fetal Bovine Serum (FBS), and antibiotics. Human cervical adenocarcinoma HeLa cells (ATCC) were cultured in Dulbecco's modified Eagle's medium (4500 mg/L glucose), 10% FBS, 1% nonessential amino acids, and antibiotics. The cell lines were maintained in standard culture conditions (37°C, and 5% CO_2).

2.5 | Cell viability assay

Cell viability was measured by 3-(4,5-dimethylthiazol-2-yl)-2,5-diphenyltetrazolium bromide (MTT, Sigma-Aldrich, St. Louis, MO) assay (Berridge & Tan, 1993). SK-N-SH and HeLa cells were seeded in 96-well plates in complete culture medium at a density of 2.0×10^4 and 0.7×10^4, respectively. The assay was performed according to the experimental procedure from our previous publication (Kavetsou et al., 2017). Two independent experiments were done in triplicate for each compound and the IC_{50} values were calculated using the GraphPad Prism software.

2.6 | General procedure for the synthesis of acetyloxy-coumarins 3a-3f

A mixture of the appropriate phenylacetic acid (3.72 mmol) and 2′,6′-dihydroxyacetophenone (3.90 mmol) in the presence of triethylamine (11.5 mmol) in acetic anhydride (4.1 ml) was refluxed for 3 hr. After the completion of the reaction, water was added and the mixture was extracted with dichloromethane. The organic phase was separated, dried over anhydrous Na_2SO_4, filtered, and evaporated to give the crude product. The products were purified by recrystallization from methanol and dichloromethane.

5-acetyloxy-3-(4-bromo-phenyl)-4-methyl-chromen-2-one (3a): white powder, yield: 50%, m.p.: 173–175 °C, ^{1}H NMR (600 MHz, $CDCl_3$): δ (ppm) 7.59 (d, J = 7.8 Hz, 2H, H-3′, H-5′), 7.53 (t, J = 8.4 Hz, 1H, H-7), 7.30 (dd, J = 8.4 Hz, J = 1.2 Hz, 1H, H-8), 7.15 (d, J = 7.8 Hz, 2H, H-2′ & H-6′), 6.99 (dd, J = 8.4 Hz, J = 1.2 Hz, 1H, H-6), 2.36 (s, 3H, 4-CH_3), 2.35(s, 3H, 5-CH_3CO), ^{13}C NMR (150 MHz, $CDCl_3$) δ (ppm) 169.28, 159.87, 153.84, 148.10, 146.80, 133.35, 131.96, 131.86, 131.17, 128.02, 122.84, 120.06, 115.42, 114.51, 21.55, 20.40.

HRMS calcd for $C_{18}H_{14}O_4Br$ $(M + H)^+$: m/z: 373.0070, found: 373.0069.

5-acetyloxy-3-(2-bromo-phenyl)-4-methyl-chromen-2-one (3b): white powder, yield: 43%, m.p.: 118–120°C, ^{1}H NMR (600 MHz, $CDCl_3$): δ (ppm) 7.69 (d, J = 7.8 Hz, 1H, H-3′), 7.54 (t, J = 7.8 Hz, 1H, H-7), 7.41 (t, J = 7.8 Hz, 1H, H-5′), 7.32 (d, J = 8.4 Hz, 1H, H-6′), 7.28 (t, J = 7.8 Hz, 1H, H-4′), 7.23 (d, J = 7.9 Hz, 1H, H-8), 7.01 (d, J = 8.4 Hz, 1H, H-6), 2.35 (s, 3H, 4-CH_3), 2.28 (s, 1H, 5-CH_3CO), ^{13}C NMR (150 MHz, $CDCl_3$): δ (ppm) 169.22, 159.05, 154.10, 148.16, 147.84, 135.62, 133.09, 131.41, 130.16, 131.21, 128.45, 127.91, 124.35, 119.98, 115.45, 114.15, 21.52, 19.88.

HRMS calcd for $C_{18}H_{14}O_4Br$ $(M + H)^+$: m/z: 373.0070, found: 373.0069.

5-acetyloxy-3-(4-nitro-phenyl)-4-methyl-chromen-2-one (3c): brown powder, yield: 42%, m.p.: 193–195°C, ^{1}H NMR (600 MHz, $CDCl_3$): δ (ppm) 8.32 (d, J = 8.4 Hz, 2H, H-3′ & H-5′), 7.57 (t, J = 8.4 Hz, 1H, H-7), 7.48 (d, J = 9 Hz, 2H, H-2′ & H-6′), 7.32 (dd, J = 8.4 Hz, J = 0.6 Hz, 1H, H-8), 7.02 (dd, J = 8.4 Hz, J = 0.6 Hz, 1H, H-6), 2.37 (s, 3H, 4-CH_3), 2.36 (s, 3H, 5-CH_3CO), ^{13}C NMR (150 MHz, $CDCl_3$): δ (ppm) 169.19, 159.41, 153.92, 148.28, 147.89, 147.60, 141.36, 131.72, 131.48, 127.07, 123.91, 120.30, 115.50, 114.19, 21.55, 20.46.

HRMS calcd for $C_{18}H_{14}O_6N$ $(M + H)^+$: m/z: 340.0816, found: 340.0814.

5-acetyloxy-4-methyl-3-phenyl-chromen-2-one (3d): white powder, yield: 46%, m.p.: 147–149 °C (lit. m.p. 150–152°C (Seshadri, 1952)), ^{1}H NMR (600 MHz, $CDCl_3$): δ (ppm) 7.50 (t, J = 8.4 Hz, 1H, H-7), 7.44 (t, J = 7.2 Hz, 2H, H-3′ & H-5′), 7.39 (t, J = 7.2 Hz, 1H, H-4′), 7.29 (d, J = 8.4 Hz, 1H, H-8), 7.25 (d, J = 6.6 Hz, 2H, H-2′ & 6′), 6.97 (d, J = 8.4 Hz, 1H, H-6), 2.34 (s, 6H, 4-CH_3 & 5-CH_3CO).

5-acetyloxy-3-(2-methoxy-phenyl)-4-methyl-chromen-2-one (3e): white powder, yield: 50%, m.p.: 150–152°C, ^{1}H NMR (600 MHz, $CDCl_3$): δ (ppm) 7.49 (t, J = 8.4 Hz, 1H, H-7), 7.39 (pseudotriplet, H-4′), 7.29 (d, J = 8.4 Hz, 1H, H-8), 7.14 (d, J = 7.2 Hz, 1H, H-6), 7.04 (t, J = 7.2 Hz, 1H, H-3′), 6.98 (m, 2H, H-2′ & H-5′), 3.78 (s, 3H, 2'-OCH_3), 2.34 (s, 3H, 4-CH_3), 2.29 (s, 3H, 5-CH_3CO), ^{13}C NMR (75 MHz, $CDCl_3$): δ (ppm) 169.34, 159.73, 157.23, 154.01, 147.90, 147.12, 131.22, 130.60, 130.17, 126.08, 123.39, 120.85, 119.72, 115.34, 114.63, 111.33, 55.73, 21.55, 19.99.

HRMS calcd for $C_{19}H_{17}O_5$ $(M + H)^+$: m/z: 325.1071, found: 325.1072.

5-acetyloxy-3-(4-methoxy-phenyl)-4-methyl-chromen-2-one (3f): yellow powder, yield: 52%, m.p.: 153–155°C, ^{1}H NMR (600 MHz, $CDCl_3$): δ (ppm) 7.50 (t, J = 8.1 Hz, 1H, H-7), 7.29 (d, J = 7.8 Hz, 1H, H-8), 7.21 (d, J = 8.7 Hz, 2H, H-2 & H-6′), 6.99 (d, J = 8.4 Hz, 2H, H-3′ & H-5′), 6.98 (d, J = 8.4 Hz, 1H, H-6), 3.88 (s, 3H, 4'-OCH_3), 2.40 (s, 3H, 4-CH_3), 2.39 (s, 3H, 5-CH_3CO), ^{13}C NMR (75 MHz, $CDCl_3$): δ (ppm) 169.35, 160.45, 159.67, 153.75, 147.95, 146.13, 131.41, 130.71, 128.82, 126.51, 119.86, 115.33, 114.82, 114.16, 55.44, 21.55, 20.43.

HRMS calcd for $C_{19}H_{17}O_5$ $(M + H)^+$: m/z: 325.1071, found: 325.1073.

2.7 | General procedure for the synthesis of hydroxy-coumarins 4a-4f

A mixture of the appropriate 5-acetyloxy-coumarin (1.50 mmol) and hydrazine monohydrate (7.48 mmol) in methanol (24.3 ml) was stirred at 42°C for 1–2 hr. After the completion of the reaction, water was added and the mixture was then extracted with ethyl acetate. The organic phase was separated, dried over anhydrous Na_2SO_4, filtered, and evaporated to give the crude product. The products were purified

by recrystallization from dichloromethane and methanol. The yields are reported by calculating the amount of the recrystallized product.

5-hydroxy-3-(4-bromo-phenyl)-4-methyl-chromen-2-one (4a): yellow powder, yield: 40%, m.p.: 228°C (decomp.), ^{1}H NMR (600 MHz, DMSO-d_6): δ (ppm) 10.72 (br, 1H, 5-OH), 7.64 (d, J = 8.4 Hz, 2H, H-3′ & H-5′), 7.39 (t, J = 8.4 Hz, 1H, H-7), 7.25 (d, J = 7.8 Hz, 2H, H-2′ & H-6′), 6.82 (t, J = 8.4 Hz, 2H, H-6 & H-8), 2.40 (s, 3H, 4-CH_3), ^{13}C NMR (150 MHz, DMSO-d_6): δ (ppm) 159.51, 157.12, 153.77, 149.99, 134.50, 132.56, 131.88, 131.19, 123.67, 121.05, 111.63, 109.11, 107.09, 21.31, 21.29.

5-hydroxy-3-(2-bromo-phenyl)-4-methyl-chromen-2-one (4b): yellow powder, yield: 41%, m.p.: 264–265°C, ^{1}H NMR (600 MHz, CD_3OD): δ (ppm) 7.71 (d, J = 7.8 Hz, 1H, H-3′), 7.45 (t, J = 7.2 Hz, 1H, H-7), 7.39 (t, J = 7.8 Hz, 1H, H-5′), 7.32 (t, J = 7.8 Hz, 1H, H-4′), 7.29 (d, J = 7.8 Hz, 1H, H-6′), 6.85 (d, J = 7.8 Hz, 1H, H-8), 6.78 (d, J = 8.4 Hz, 1H, H-6), 2.41 (s, 3H, 4-CH_3), ^{13}C NMR (150 MHz, DMSO-d_6): δ (ppm) 158.65, 157.23, 153.96, 150.71, 136.18, 132.38, 132.13, 131.98, 130.0, 127.99, 124.35, 124.08, 111.68, 108.66, 107.15, 20.74.

HRMS calcd for $C_{16}H_{12}O_3Br$ $(M + H)^+$: m/z: 390.9964, found: 330.9961.

5-hydroxy-4-methyl-3-(4-nitro-phenyl)-chromen-2-one (4c): brown powder, yield: 56%, m.p.: 282°C (decomp.), ^{1}H NMR (600 MHz, DMSO-d_6): δ (ppm) δ (ppm) 10.76 (br, 1H, 5-OH), 8.30 (d, J = 8.4 Hz, 2H, H-3′ & H-5′), 7.61 (d, J = 8.4 Hz, 2H, H-2′ & H-6′), 7.42 (t, J = 7.8 Hz, 1H, H-7), 6.84 (t, J = 9 Hz, 2H, H-6&H-8), 2.41 (s, 3H, 4-CH_3), ^{13}C NMR (75 MHz, DMSO-d_6): δ (ppm) 159.74, 157.05, 153.79, 149.62, 135.24, 131.71, 130.24, 128.23, 127.56, 124.85, 111.57, 109.20, 10,710, 21.32.

HRMS calcd for $C_{16}H_{10}O_5N$ $(M-H)^-$: m/z: 296.0564, found: 296.0555.

5-hydroxy-4-methyl-3-phenyl-chromen-2-one (4d): white powder, yield: 50%, m.p.: 277–278°C (lit. m.p. 276–278°C (Seshadri, 1952)), ^{1}H NMR (600 MHz, DMSO-d_6): δ (ppm) 10.65 (br, 1H, 5-OH), 7.44 (t, J = 7.8 Hz, 2H, H-3′ & H-5′), 7.38 (t, J = 7.8 Hz, 2H, H-7 & H-4′), 7.27 (d, J = 7.2 Hz, 2H, H-2′ & H-6′), 6.82 (t, J = 7.8 Hz, 2H, H-6 & H-8), 2.40 (s, 3H, 4-CH_3), ^{13}C NMR (75 MHz, DMSO-d_6): δ (ppm) 159.21, 157.29, 153.86, 150.59, 146.90, 142.52, 132.22, 131.97, 123.29, 123.03, 111.71, 108.94, 107.13, 21.37.

5-hydroxy-3-(2-methoxy-phenyl)-4-methyl-chromen-2-one (4e): yellow powder, yield: 45%, m.p.: 252–255°C, ^{1}H NMR (600 MHz, DMSO-d_6): δ (ppm) 10.65 (br, 1H, 5-OH), 7.38 (m, 2H, H-2′ & H-5′), 7.14 (dd, J = 7.2 Hz, J = 1.2 Hz, 1H, H-6), 7.09 (d, J = 8.4 Hz, 1H, H-8), 7.01, (t, J = 7.2 Hz, 1H, H-7), 6.8 (t, J = 7.2 Hz, 2H, H-3′ & H-4′), 3.72 (s, 3H, 2'-OCH_3), 2.32 (s, 3H, 4-CH_3), ^{13}C NMR (150 MHz, DMSO-d_6): δ (ppm) 159.14, 156.92, 156.86, 153.81, 150.07, 131.58, 131.23, 129.49, 123.80, 121.74, 120.32, 111.47, 111.28, 109.02, 107.03, 55.42, 20.86.

HRMS calcd for $C_{17}H_{13}O_4$ $(M-H)^-$ m/z: 281.0819, found: 281.0808.

5-hydroxy-3-(4-methoxy-phenyl)-4-methyl-chromen-2-one (4f): yellow powder, yield: 62%, m.p.: 220–222°C, ^{1}H NMR (300 MHz, DMSO-d_6): δ (ppm) 7.33 (t, J = 8.9 Hz, 1H, H-7), 7.16 (d, J = 8.7, 2H, H-2′ & H-6′), 6.96 (d, J = 8.7 Hz, 2H, H-3′ & H-5′), 6.78, (dd, J = 8.1 Hz, J = 1.5 Hz, 2H, H-6 & H-8), 3.79 (s, 3H, 4'-OCH_3), 2.41 (s, 3H, 4-CH_3), ^{13}C NMR (75 MHz, DMSO-d_6): δ (ppm) 161.64, 158.65, 156.90, 153.66, 149.35, 134.47, 131.51, 127.11, 124.51, 113.30, 111.51, 109.29, 107.02, 55.10, 21.33.

HRMS calcd for $C_{17}H_{15}O_4$ $(M + H)^+$: m/z: 283.0965, found: 283.0961.

2.8 | General procedure for the synthesis of prenyloxy-coumarins 5a-5f

A mixture of the appropriate 5-hydroxy-coumarin (0.52 mmol) and geranyl-bromide (0.62 mmol) in acetone (19.9 ml) in the presence of potassium carbonate (K_2CO_3 0.52 mmol) was refluxed overnight. After the completion of the reaction, potassium carbonate was filtered off, washed with acetone and the filtrate was evaporated under reduced pressure. The residue was then purified by flash column chromatography (petroleum ether/ethyl acetate 9:1).

5-geranyloxy-3-(4-bromo-phenyl)-4-methyl-chromen-2-one (5a): yellow powder, yield: 89%, m.p.: 91–94°C, ^{1}H NMR (600 MHz, $CDCl_3$): δ (ppm) 7.57 (d, J = 8.4 Hz, 2H, H-3′ & H-5′), 7.42 (t, J = 8.4 Hz, 1H, H-7), 7.16 (d, J = 8.4 Hz, 2H, H-2′ & H-6′), 6.97 (d, J = 8.4 Hz, 1H, H-8), 6.77 (d, J = 8.4 Hz, 1H, H-6), 5.49 (t, J = 6.6 Hz, 1H, H-2″), 5.06 (t, J = 6.6 Hz, 1H, H-6″), 4.63 (d, J = 6.6 Hz, 2H, H-1″), 2.46 (s, 3H, 4-CH_3), 2.10 (m, 4H, H-4″ & H-5″), 1.74 (s, 3H, 3″-CH_3), 1.65 (s, 3H, 8″-CH_3), 1.59 (s, 3H, 7″-CH_3), ^{13}C NMR (150MHz, $CDCl_3$): δ (ppm) 160.68, 157.91, 154.39, 150.49, 142.14, 134.24, 132.27, 132.02, 131.87, 131.58, 131.42, 125.41, 123.89, 123.42, 122.27, 118.80, 111.35, 109.76, 107.72, 107.50, 66.12, 39.56, 26.35, 22.38, 22.03.

HRMS calcd for $C_{26}H_{28}O_3Br$ $(M + H)^+$: m/z: 467.1216, found: 467.1211.

5-geranyloxy-3-(2-bromo-phenyl)-4-methyl-chromen-2-one (5b): yellow oily product, yield: 85%, ^{1}H NMR (600 MHz, $CDCl_3$): δ (ppm) 7.69 (d, J = 7.8 Hz, 1H, H-3′), 7.43 (t, J = 8.4 Hz, 1H, H-7), 7.39 (t, J = 7.8 Hz, 1H, H-5′), 7.25 (m, 2H, H-4′ & H-6′), 6.99 (d, J = 8.4 Hz, 1H, H-8), 6.78 (d, J = 8.4 Hz, 1H, H-6), 5.49 (t, J = 6.0 Hz, 1H, H-2″), 5.06 (t, J = 6.6 Hz, 1H, H-6″), 4.63 (d, J = 6.6 Hz, 2H, H-1″), 2.38 (s, 3H, 4-CH_3), 2.08 (m, 4H, H-4″ & H-5″), 1.74 (s, 3H, 3″-CH_3), 1.64 (s, 3H, 8″-CH_3), 1.58 (s, 3H, 7″-CH_3), ^{13}C NMR (75MHz, $CDCl_3$): δ (ppm) 159.94, 158.05, 154.70, 151.50, 142.12, 136.47, 133.01, 132.07, 131.73, 131.68, 129.79, 127.82, 125.94, 124.78, 123.66, 118.76, 111.03, 109.84, 107.57, 66.11, 39.55, 26.34, 25.80, 21.60, 17.84, 16.80.

HRMS calcd for $C_{26}H_{28}O_3Br$ $(M + H)^+$: m/z: 467.1216, found: 467.1216.

5-geranyloxy-4-methyl-3-(4-nitro-phenyl)-chromen-2-one (5c): yellow powder, yield: 64%, m.p.: 104–107°C, ^{1}H NMR (600 MHz, $CDCl_3$): δ (ppm) 8.30 (d, J = 8.4 Hz, 2H, H-3′ & H-5′), 7.46 (m, 3H, H-2′ & H-6′ & H-7), 6.99 (d, J = 7.8 Hz, 1H, H-8), 6.80 (d, J = 8.4 Hz, 1H, H-6), 5.49 (t, J = 6.6 Hz, 1H, H-2″), 5.06 (br, 1H, H-6″), 4.65 (d, J = 6.6 Hz, 2H, H-1″), 2.47 (s, 3H, 4-CH_3), 2.10 (m, 4H, H-4″ & H-5″),

1.75 (s, 3H, 3″-CH_3), 1.65 (s, 3H, 8″-CH_3), 1.59 (s, 3H, 7″-CH_3), ^{13}C NMR (150 MHz, $CDCl_3$) δ (ppm) 160.19, 158.09, 154.52, 151.24, 147.59, 142.42, 142.38, 132.22, 132.08, 131.69, 127.73, 124.45, 123.77, 123.65, 123.60, 118.60, 111.04, 109.78, 107.80, 66.22, 39.55, 26.33, 25.79, 22.27, 17.83, 16.80.

HRMS calcd for $C_{26}H_{28}O_5N$ $(M + H)^+$: m/z: 434.1962, found: 434.1962.

5-geranyloxy-4-methyl-3-phenyl-chromen-2-one (5d): yellow gummy solid, yield: 95%, ^{1}H NMR (600 MHz, $CDCl_3$): δ (ppm) 7.40 (m, 4H, H-7 & H-3′& H-4′ & H-5′), 7.28 (br, 2H, H-2′ & H-6′), 6.98 (d, *J* = 8.4 Hz, 1H, H-8), 6.77 (d, *J* = 8.4 Hz, 1H, H-6), 5.49 (t, *J* = 6 Hz, 1H, H-2″), 5.06 (br, 1H, H-6″), 4.63 (d, *J* = 6.6 Hz, 2H, H-1″), 2.46 (s, 3H, 4-CH_3), 2.10 (m, 4H, H-4″ & H-5″), 1.74 (s, 3H, 3″-CH_3), 1.65 (s, 3H, 8″-CH_3), 1.59 (s, 3H, 7″-CH_3), ^{13}C NMR (150 MHz, $CDCl_3$): δ (ppm) 160.97, 157.89, 154.44, 150.10, 142.04, 135.36, 132.07, 131.34, 130.30, 128.57, 128.02, 127.75, 126.62, 123.70, 123.66, 118.87, 111.57, 109.77, 107.55, 66.10, 39.57, 26.36, 25.79, 22.17, 17.85, 16.79.

HRMS calcd for $C_{26}H_{29}O_3$ $(M + H)^+$: m/z: 389.2111, found: 389.2117.

5-geranyloxy-3-(2-methoxy-phenyl)-4-methyl-chromen-2-one (5e): white powder, yield: 96%, m.p.: 85–87°C, ^{1}H NMR (600 MHz, $CDCl_3$): δ (ppm) 7.37 (m, 2H, H-7 & H4'), 7.15 (dd, *J* = 7.8 Hz, *J* = 1.8 Hz, 1H, H-5′), 7.03 (t, *J* = 7.8 Hz, 1H, H-3′), 6.98 (m, 2H, H-6 & H-8), 6.75 (d, *J* = 7.8 Hz, 1H, H-2′), 5.49 (t, *J* = 6.6 Hz, 1H, H-2″), 5.06 (t, *J* = 6.6 Hz, 1H, H-6″), 4.62 (d, *J* = 6.6 Hz, 2H, H-1″), 3.78 (s, 3H, 2'-OCH_3), 2.09 (m, 4H, H-4″ & H-5″), 1.74 (s, 3H, 3″-CH_3), 1.65 (s, 3H, 8″-CH_3), 1.59 (s, 3H, 7″-CH_3), ^{13}C NMR (75MHz, $CDCl_3$): δ (ppm) 160.57, 157.79, 157.39, 154.58, 150.79, 141.83, 132.03, 131.49, 131.11, 129.74, 124.28, 123.70, 123.38, 120.82, 118.97, 11.55, 111.32, 109.77, 107.38, 66.04, 55.76, 39.55, 26.35, 25.80, 21.68, 17.85, 16.78.

HRMS calcd for $C_{27}H_{31}O_4$ $(M + H)^+$: m/z: 419.2217, found: 419.2216.

5-geranyloxy-3-(4-methoxy-phenyl)-4-methyl-chromen-2-one (5f): yellow powder, yield.: 56%, m.p.: 77°C, ^{1}H NMR (600 MHz, $CDCl_3$): δ (ppm) 7.39 (t, *J* = 6.6 Hz, 1H, H-7), 7.20 (d, *J* = 8.4 Hz, 2H, H-2′ & H-6′), 6.97 (d, *J* = 8.4 Hz, 2H, H-3′ & H-5′), 6.96 (d, *J* = 7.2 Hz, 1H, H-8), 6.76 (d, *J* = 8.4 Hz, 1H, H-6), 5.50 (t, *J* = 6.0 Hz, 1H, H-2″), 5.06 (d, *J* = 6.0 Hz, 2H, H-6″), 4.62 (d, *J* = 6.6 Hz, 2H, H-1″), 3.84 (s, 3H, 4'-OCH_3), 2.48 (s, 3H, 4-CH_3), 2.10 (m, 4H, H-4″ & H-5″), 1.74 (s, 3H, 3″-CH_3), 1.65 (s, 3H, 7″-CH_3), 1.59 (s, 3H, 8″-CH_3), ^{13}C NMR (75MHz, $CDCl_3$): δ (ppm) 161.35, 159.32, 157.78, 154.26, 150.04, 141.97, 132.05, 131.55, 131.22, 127,40, 126.18, 118.92, 118.87, 114.04, 111.66, 109.70, 107.51, 66.07, 55.40, 39.55, 26.34, 25.80, 22.23, 17.84, 16.79.

HRMS calcd for $C_{27}H_{31}O_4$: m/z: 419.2217, found: 419.2214.

3 | RESULTS AND DISCUSSION

3.1 | Chemistry

Our latest research focuses on the design, synthesis, and bioactivity evaluation of a series of 3-aryl coumarin analogues as well as a series of prenyloxy derivatives of the natural compound umbelliferone (e.g., auraptene) (Kavetsou et al., 2017; Roussaki et al., 2010; Roussaki et al., 2014). The promising results of these works in combination with the literature data (Dos Santos Nascimento et al., 2015; Ibrar, Shehzadi, Saeed, & Khan, 2018; Jabbari, Mousavian, Seyedi, Bakavoli, & Sadeghian, 2017), which reveal the role of the phenyl group at the prenylated coumarin's skeleton (Wiart, 2013), as well as the role of different substitutions on the phenyl group of an acetyloxy coumarin (Musa, Latinwo, Joseph, & Badisa, 2017), led us to design new series of coumarin analogues which combine the 3-aryl substituent and acetyloxy-/hydroxy- or geranyloxy moiety in order to investigate the effect of the presence of these groups on the biological activity (Scheme 1).

In order to efficiently synthesize the target compounds, a series of three reactions was performed (Scheme 2): first, the 5-acetyloxy-coumarins (**3a-3f**) were synthesized via a Perkin-Oglialoro condensation reaction between an appropriately substituted phenylacetic acid (**1a-1f**) and 2′,6′-dihydroxyacetophenone (**2**) in acetic anhydride in the presence of a catalytic amount of triethylamine. Subsequently, the acetyl group was removed using hydrazine monohydrate in methanol leading to 5-hydroxy-compounds (**4a-4f**). The final 5-geranyloxy-coumarins (**5a-5f**) were obtained by alkylation of the 5-hydroxy-coumarins with geranyl bromide and potassium carbonate (K_2CO_3) in acetone. All the products were purified using flash column chromatography or recrystallization and were structurally identified using ^{1}H and ^{13}C NMR spectroscopy and HR-MS spectrometry. Lipophilicity values were calculated in silico.

3.2 | Antioxidant activity evaluation

The in vitro antioxidant activity of the synthesized molecules was evaluated as their ability to inhibit lipid peroxidation (LP) (AAPH assay) and the results are presented in Table 1.

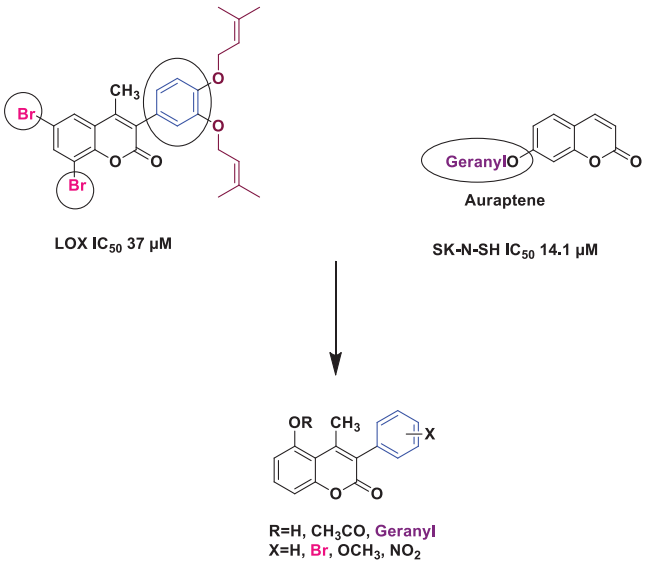

SCHEME 1 Key structural features for the synthesis of the new 3-aryl-5-substituted coumarin analogues (Kavetsou et al., 2017; Roussaki et al., 2014)

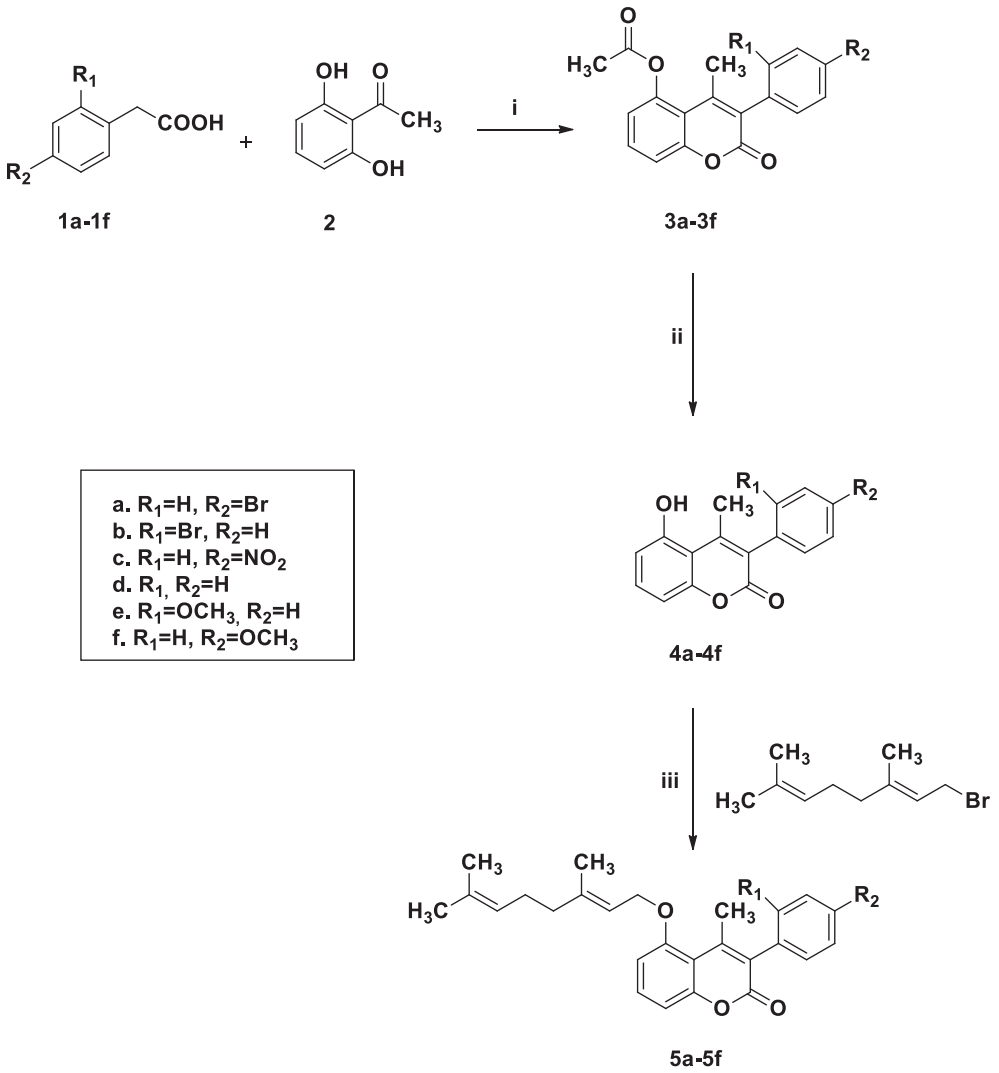

SCHEME 2 Reagents and conditions: (i) Et_3N, AC_2O, reflux, 3 hr, (ii) $NH_2NH_2.H_2O$, MeOH, 42°C, 1.5 hr, and (iii) K_2CO_3, acetone, reflux, 24 hr

Among the 5-acetyloxy-coumarins (**3a-3f**), only compounds **3a** (87.7%) and **3b** (100%) that contain a bromo-substituent on the 3-phenyl ring were found to be active. Removal of the acetyl group (compounds **4a** and **4b**) as well as alkylation of the OH group (compounds **5a** and **5b**) led to analogues with decreased activity. In addition, compound **3a**, bearing an acetyloxy-group at position 5 of the coumarin core, possesses enhanced antioxidant activity compared with the 3-(4-bromo-phenyl)-4-methyl-coumarin analogue studied in our previous work (36% LP inhibition) (Roussaki et al., 2010).

Moreover, as long as 5-hydroxy-coumarins (**4a-4f**) are concerned, the most potent LP inhibitor was compound **4d** (100%) indicating that the absence of substitution on the phenyl group favors the bioactivity in these series of compounds. Meanwhile, the presence of a hydroxyl group at position 5 of the coumarin scaffold turned an inactive compound (**3d**) into a strong LP inhibitor (**4d**).

Among the 5-geranyloxy-analogues, compound **5c**, bearing a nitro-substituent, exhibited significant LP inhibition (93.1%), higher than the 5-hydroxy-analogue, **4c** (24%), whereas the 5-acetyloxy-analogue, **3c**, showed no activity. In this case, the presence of a geranyloxy moiety enhanced bioactivity not only in comparison with the acetyloxy- and hydroxy- derivatives, but also compared with the 5-unsubstituted analogue (4-methyl-3-(4-nitro-phenyl)-coumarin) which was found to be inactive (Roussaki et al., 2010). Lipophiicity, determined theoretically as *c* log *p* values does not seem to influence the antioxidant activity. Compounds presenting the highest activities do not show the highest *c* log *p* values (e.g., **3b, 4d**, and **5c**) (Biobyte Corp. C-QSAR Database, n.d.; Pontiki & Hadjipavlou-Litina, 2008).

3.3 | Soybean lipoxygenase inhibitory activity evaluation

It is well-known that lipoxygenases' activity, such as 15-LOX, is closely related with inflammation responses, as previously described. In addition, its metabolism products, such as 5-HETE and LTD4, promote cancer cell proliferation and growth, although the relationship between lipoxygenases and cancer may depend on the tumor's microenvironment. On this basis, scientific research focuses on the development of 15-LOX inhibitors for the chemoprevention of different

TABLE 1 Inhibitory activity of coumarins **3a**-**5f** against: lipid peroxidation induced by AAPH (%), soybean lipoxygenase activity (IC_{50}), cell growth of SK-N-SH and HeLa cell lines (IC_{50}), and their theoretically calculated lipophilicity (*C* log *P*)

Compound	*C* log *P* (biobyte Corp. C-QSAR database)	% inhibition of LP induced by AAPH[a] (100 μM)	Inhibition of soybean lipoxygenase [b]IC_{50} (μM)	Inhibition of cell growth IC_{50} (μM)	
				SK-N-SH	HeLa
3a	4.34	88 ± 1.4*	57.5 ± 0.7*	20.2	1.8
3b	4.04	100 ± 2.3*	100 ± 1.3**	9.7	6.1
3c	3.22	NA	NA	34.4	55.4
3d	3.47	NA	NA	34.7	24.5
3e	2.84	25 ± 0.6*	NA	170.6	47.8
3f	3.40	5 ± 0.3*	NA	74.2	17.9
4a	4.78	66 ± 1.5**	NA	>500	79.1
4b	4.48	48 ± 1.1**	NA	60.5	12.8
4c	3.66	24 ± 0.9*	40 ± 1.0*	>500	104.6
4d	3.92	100 ± 3.2*	NA	380.7	37.4
4e	3.29	NA	21 ± 0.3*	>500	116.8
4f	3.85	60 ± 1.6**	NA	No	>500
5a	8.64	38 ± 1.1*	64 ± 0.8**	366.1	>500
5b	8.01	47 ± 1.4*	NA	13.6	222.0
5c	7.52	93 ± 2.8**	NA	NA	>500
5d	7.78	54 ± 1.9*	NA	35.8	60.4
5e	7.14	25 ± 0.5*	60 ± 0.9**	9.7	21.5
5f	7.70	53 ± 0.8*	10 ± 0.1*	94.8	55.0
Trolox	-	93 ± 2.6*	-	-	-
NDGA	-	-	0.45 ± 0.1*	-	-

Note: NDGA: Nordihydroguaiaretic acid. NA: No Activity under the used experimental conditions.

[a]Values are means (± *SD* < 10%) of four different determinations.

[b]For the IC_{50} determination of LOX inhibition six different concentrations were used.

*p < .05; **p < .01.

types of cancer, such as prostate and pancreatic. (Orafaie et al., 2018; Yang et al., 2013).

Soybean (*Glycine max*) LOX-1 is a 15-LOX, which has been used widely as a prototype for studying the functional and structural properties of the homologous family of lipoxygenases. The crystal structures of soybean LOX-1 and that of a rabbit 15-LOX-1-inhibitor complex in addition, to the three-dimensional models of the human 5-LOX indicated that the essential structural features of plant and animal LOXs are highly conserved (Brash, 1999; Funk, 2001).

Soybean LOX was selected in this study and the inhibitory activity of the compounds was tested and is presented in Table 1.

The most active LOX inhibitors among the 5-acetyloxy-derivatives were the bromo-substituted **3a** (IC_{50} 57.5 μM) and **3b** (IC_{50} 100 μM) analogues, while deacetylation of these compounds led to essentially lower bioactivity (**4a** and **4b**). In our previous work, 3-(4-bromo-phenyl)-4-methyl-coumarin was found to be an inactive anti-inflammatory agent. The recent results show that the insertion of an acetyloxy- group at position 5 of the coumarin scaffold (**3a**) significantly improves the activity (Roussaki et al., 2010).

Among the 5-hydroxy-coumarins, compound **4e** bearing a methoxy- group at position 2 of the 3-aryl moiety, displayed the highest LOX inhibitory activity (IC_{50} 21 μM), whereas compound **4f** possessing a methoxy- group at position 4 was inactive. It is also remarkable that the presence of a hydroxy- group at position 5 of the 4-nitro-substituted coumarin derivative (**4c**) significantly enhances soybean LOX inhibitory activity in comparison with the non hydroxy-analogue (Roussaki et al., 2010).

Regarding the geranyloxy-analogues, the most potent LOX inhibitory agent was compound **5f** (IC_{50} 10 μM), which is the best analogue among the compounds studied in this work. Coumarins **5a** and **5f** bearing a bromo or methoxy group, respectively, at position 4 on the phenyl ring were more active than the corresponding 2-substituted analogues (**5b** & **5e**), indicating that the position of the substituent is an important structural feature for LOX inhibition. As a general observation, the absence of substituents at the 3-phenyl ring leads to complete loss of activity (**3d**, **4d**, and **5d**). Lipophilicity is a physicochemical property which can be related to LOX inhibition; however, the results obtained in this study do not show this trend (Pontiki & Hadjipavlou-Litina, 2008).

Compounds **4e** and **5f** exhibited the higher IC_{50} values with low interaction with AAPH, thus showing that LOX inhibition is not always accompanied by antioxidant ability and vice versa (Curini et al., 2006).

3.4 | Cytotoxic activity evaluation

Cytotoxicity of coumarin analogues against various types of cancer cell lines stands out among their various bioactivities. In this study, the potential cytotoxicity of 18 coumarin analogues via the MTT assay using the human neuroblastoma cell line SK-N-SH and the human cervical epithelioid cell line HeLa was investigated. SK-N-SH human neuroblastoma cell line was selected to allow comparisons on the cytotoxic activity evaluation of hydroxy and oxyprenylated coumarin derivatives studied previously by our group (Kavetsou et al., 2017). Both SK-N-SH and HeLa cells have been widely used to examine the anticancer effect of bioactive agents (Akram et al., 2018; Dickens et al., 2019; Goswami et al., 2018; Park et al., 2019; Qi et al., 2019; Swift, Zhang, Trippett, & Narendran, 2019; Yen et al., 2018).

The results are presented in Table 1 and Figures 1 and 2.

Concerning the SK-N-SH neuroblastoma cell line, four of the 5-acetyloxy-coumarins presented significant activity, with IC_{50} ranging from 9.7 to 34.7 μM. Coumarins **3a** (IC_{50} 20.2 μM) and **3b** (IC_{50} 9.7 μM) bearing a bromo-substituent were the most cytotoxic.

These results could be supported by an earlier publication, in which it was recorded that the bromination of flavonoids has improved their biological properties, such as antioxidant activity and enhanced their lipophilicity and diffusion through membranes. Brominated flavonoids' metabolites may interact with signaling pathways

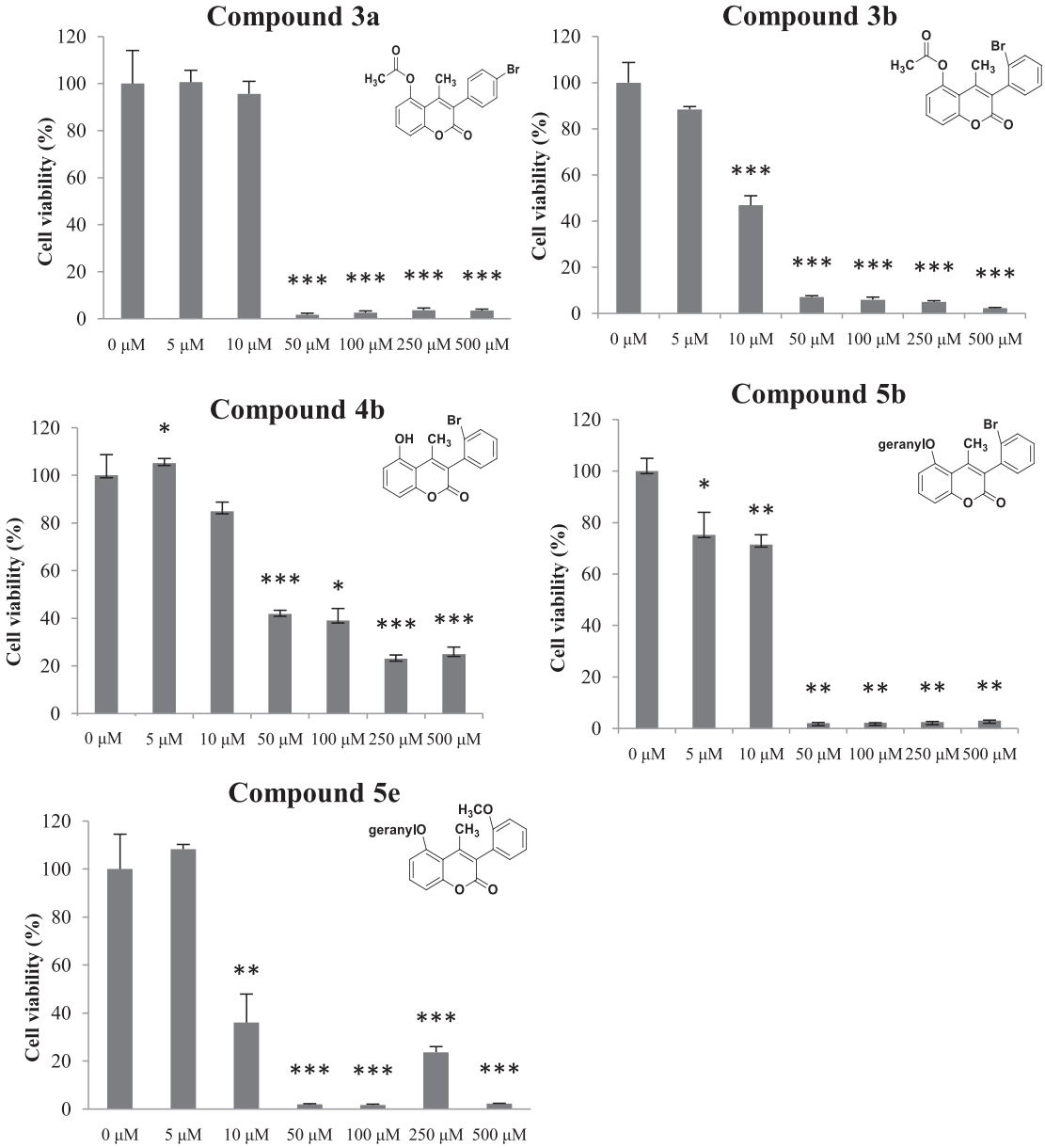

FIGURE 1 Effect of coumarin analogues **3a**, **3b**, **4b**, **5b**, and **5e** on human neuroblastoma SK-N-SH cell line. Cell viability is expressed as percent relative to the viability of control untreated cells (0 μM, incubation with the compounds dilution medium) set to 100%. Data are the means ± *SD*, **p* < .05 versus control; ***p* < .005 versus control; ****p* < .0001 versus control

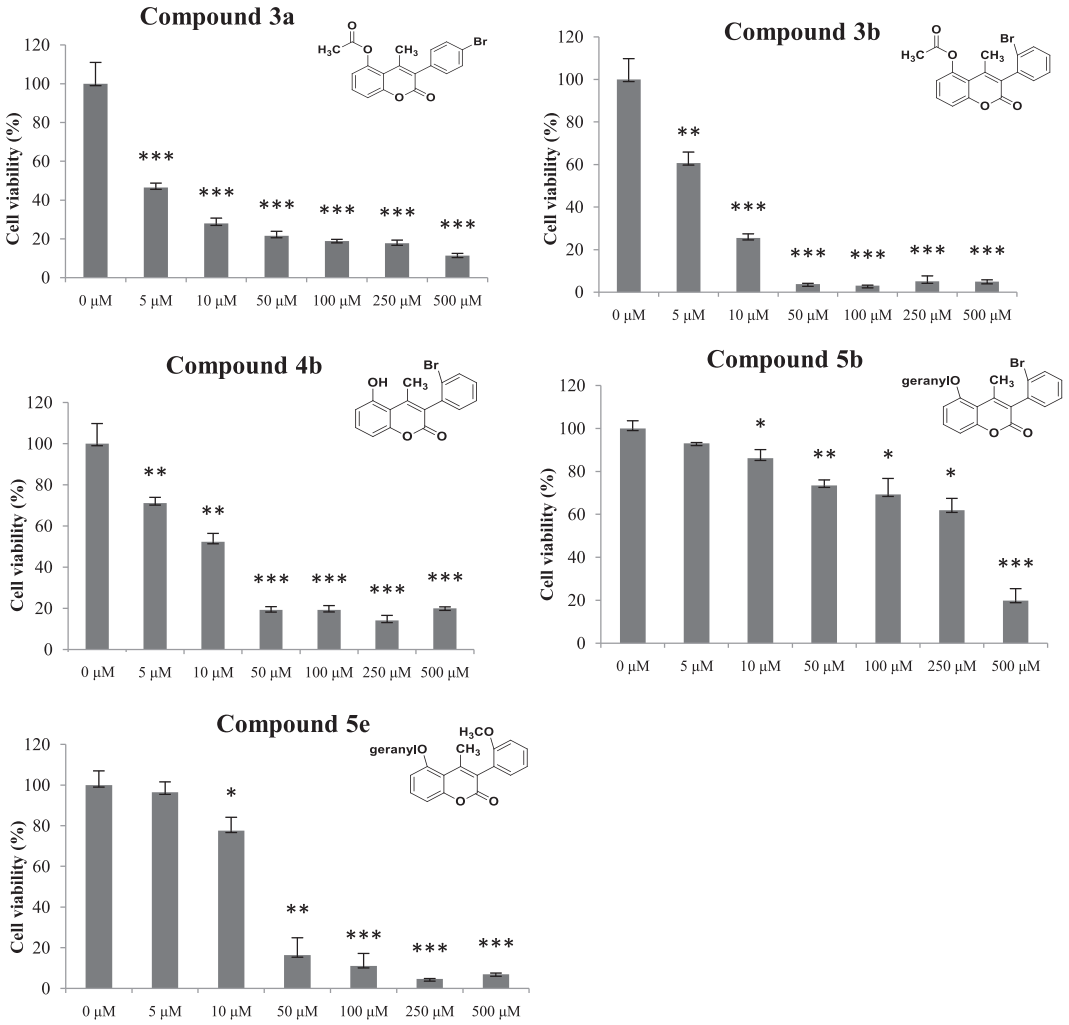

FIGURE 2 Effect of coumarin analogues **3a**, **3b**, **4b**, **5b**, and **5e** on cervical epithelioid HeLa cell line. Cell viability is expressed as percent relative to the viability of control untreated cells (0 μM, incubation with the compounds dilution medium) set to 100%. Data are the means ± *SD*, **p* < .05 versus control; ***p* < .005 versus control; ****p* < .0001 versus control

(involving cytokines and so on), closely related with inflammation and the regulation of immune response, while hypobromous acid constitutes a strong oxidant metabolite crucial for efficient cytotoxicity (Justino, Rodrigues, Florêncio, & Mira, 2009).

The presence of a methoxy substituent (**3e** & **3f**) resulted to decreased cytotoxicity. The 5-hydroxy-derivatives were found to be inactive, except for the 5-hydroxy-3-(2-bromo-phenyl)-4-methyl-coumarin (**4b**) which exhibited moderate activity (IC_{50} 60.5 μM). The influence of substitution at position 2 of the 3-aryl moiety of the 5-geranyloxy-derivatives in cytotoxicity was remarkable, since the presence of either a bromo- (**5b**, IC_{50} 13.6 μM) or a methoxy- (**5e**, IC_{50} 9.7 μM) group enhanced the cytotoxicity against SK-N-SH cells.

In regard to HeLa adenocarcinoma cell line, all the 5-acetyloxy-derivatives were significantly active (IC_{50} 1.8–55.4 μM), with the best effect presented again by compounds **3a** (IC_{50} 1.8 μM) and **3b** (IC_{50} 6.1 μM). In this cell line, it was noted that substitution at position 4 with a bromo or methoxy group on the phenyl ring of the acetyloxy-analogues favored the biological response. In all cases the 5-hydroxy-derivatives were found to be less active, although compounds **4b** (IC_{50} 12.8 μM) and **4d** (IC_{50} 37.4 μM) still presented important bioactivity. It is also noteworthy that all the 5-hydroxy-compounds were more cytotoxic against HeLa than SK-N-SH cell line. Concerning the 5-geranyloxy-analogues, coumarin **5e** was the most cytotoxic (IC_{50} 21.5 μM), while compounds **5a** and **5b** were completely inactive. It is remarkable that compound **5b**, exhibited preferential cytotoxicity against SK-N-SH (IC_{50} 13.6 μM) than HeLa line (IC_{50} 222.0 μM).

Overall, the 5-acetyloxy-coumarins, and especially the bromo-substituted derivatives (**3a** & **3b**), were found to be the most active agents against both carcinoma cell lines. The importance of the acetyloxy moiety on the cytotoxicity of coumarins has been also mentioned by other research groups (Burgess, Shah, Hough, & Hynynen, 2016; Musa et al., 2017). More specifically, in the work of Raj et al., the presence of the acetyloxy group at positions 7 and 8 on the 4-methyl-coumarin skeleton has been shown to significantly inhibit

the AFB_1-induced apoptosis (Raj et al., 2001). In the work of Musiliyu *A. Musa* et al. it was found that 7,8-diacetyloxy-3-(4-nitrophenyl)-coumarin and 7,8-diacetyloxy-3-(4-methoxyphenyl)-coumarin presented remarkable cytotoxicity against various cancer cell lines (PC 3, MDA-MB-231) (Musa et al., 2017; Musa, Latinwo, Virgile, Badisa, & Gbadebo, 2015).

Recent research shows that treatment of cervical carcinoma cells with a LOX inhibitor also inhibits their invasion and migration capacities (Yang et al., 2013). Such observations are in accordance with the combined anti-inflammatory and cytotoxic activity exhibited by compounds **3a** and **3b** against HeLa cancer cells, rendering them powerful and promising multi-targeting agents.

All in all, substitution of the coumarin scaffold with a bromine as well as an acetyloxy-moiety seems to enhance the combined bioactivity of coumarins.

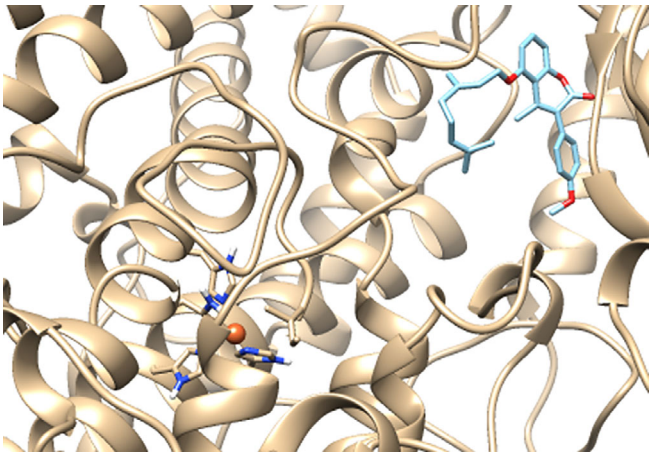

FIGURE 3 Docking orientation of **5f** (depicted in turquoise) bound to soybean lipoxygenase (LOX-1)

3.5 | Molecular docking simulations for soybean lipoxygenase

For the docking studies of soybean lipoxygenase (SLOX-1), 3PZW was selected. UCSF Chimera was used for the visualization of the protein (PDB code: 3PZW) (Pettersen et al., 2004).The above protein was prepared for docking studies by removing water molecules, adding missing residues with Modeler (Fiser & Šali, 2003), adding hydrogen atoms and AMBER99SB-ILDN charges and setting the iron charge to +2.0, with no restraint applied to the iron atom and the ligands.

OpenBabel was used to generate and minimize Ligand 3D coordinates (O'Boyle et al., 2011) using the MMFF94 force field (Halgren, 1996) while ACPYPE (AnteChamberPYthon Parser interfacE) (Sousa da Silva & Vranken, 2012) was used to generate ligand topologies and parameters using Antechamber (Wang, Wang, Kollman, & Case, 2006). Energy minimizations were accomplished using the AMBER99SB-ILDN force field (Lindorff-Larsen et al., 2010) with GROMACS 4.6.5 (Hess, Kutzner, van der Spoel, & Lindahl, 2008) as the molecular dynamics simulation toolkit. Docking studies were executed with AutoDockVina (1.1.2) (Trott & Olson, 2010) using a grid box of size 100 Å, 70 Å, and 70 Å in X, Y, and Z dimensions for SLOX-1. UCSF-Chimera was applied for the generation of docking input files and analysis of the obtained docking results. Docking was carried out with an exhaustiveness value of 10 and a maximum output of 20 docking modes SLOX-1.

3.6 | Molecular modeling of the synthesized derivatives in soybean LOX

All the synthesized compounds have been studied with in silico docking. The molecular modeling evaluation provided useful interpretation of the experimental results. The preferred docking pose in soybean LOX (PDB code: 3PZW) for the most potent derivative **5f,** shown in Figure 3, has a high AutoDockVina score (−10.5) (Figure 3). From this study, it can be concluded that the novel derivatives present allosteric interactions with the enzyme. Additionally, it seems that **5f** accommodates the extensively hydrophobic cavity close to the active site with possible hydrophobic interactions (π-π stacking). The inhibitory activity of **5f** is possible due to the obstruction of substrates to reach the active site of LOX based on the fact that lipoxygenation, occurs via a carbon-centered radical on a lipid chain and the majority of strong LOX-inhibitors are antioxidants or free radical scavengers (Denisov & Afanas'ev, 2005).

3.7 | Drug-likeness studies

The drug likeness of the derivatives was determined from the theoretical calculation of various molecular properties, for example, partition coefficient (log *P*), topological polar surface area (TPSA), hydrogen bond donors and acceptors, rotatable bonds, number of atoms, and molecular weight. The violations of Lipinski's rule of five were also considered (Lipinski, Lombardo, Dominy, & Feeney, 1997; Molinspiration (http://www.molinspiration.com//cgi-bin/properties) (Table 2). All the compounds have a molecular weight less than 500. Thus, these molecules could be easily transported, diffused, and absorbed. The theoretically calculated lipophilicity log *P* values of series **3a**-**3f** and **4a**-**4f** were found to be less than 5 and are in agreement to Lipinski's rule of five, suggesting satisfactory permeability across the cell membrane. This was not found for compounds of series **5a**-**5f** which have log *P* values more than 5. Counting the number of hydrogen bond acceptors (O and N atoms) and the number of hydrogen bond donors (NH and OH) in the synthesized compounds, it seems that both properties follow the Lipinski's rule of five (less than 10 and 5, respectively). The examined derivatives seem to be orally active in accordance to Lipinski's rule of five. The hydrogen bonding of the compounds is highly correlated to the TPSA. This property is used as a significant indicator of the bioavailability of a bioactive molecule. The TPSA of the derivatives was observed in the range of

TABLE 2 Molecular properties prediction-Lipinski "Rule of five"

Compd.	mi log *P*[a]	TPSA[b]	No. of atoms	No. of O and N[c]	No. of OH and NH[d]	No. of violations	No. of rotational bonds[e]	Volume[f]	MW[g]	log BB[h]
3a	4.34	56.52	23	4	0	0	3	278.97	373.20	0.2715
3b	4.38	56.52	23	4	0	0	3	278.97	373.20	0.2777
3c	3.58	102.34	25	7	0	0	4	284.42	339.30	−0.3045
3d	3.62	56.52	22	4	0	0	3	261.08	294.31	0.1599
3e	3.63	65.75	24	5	0	0	4	286.63	324.33	0.06915
3f	3.67	65.75	24	5	0	0	4	286.63	324.33	0.07535
4a	4.66	50.44	20	3	1	0	1	242.46	331.17	0.3819
4b	4.61	50.44	20	3	1	0	1	242.46	331.17	0.37415
4c	3.81	96.26	22	6	1	0	2	247.91	297.27	−0.20805
4d	3.85	50.44	19	3	1	0	1	224.57	252.27	0.25635
4e	3.85	59.67	21	4	1	0	2	250.12	282.30	0.16405
4f	3.90	59.67	21	4	1	0	2	250.12	282.30	0.1718
5a	8.37	39.45	30	3	0	1	7	398.35	467.40	1.06685
5b	8.34	39.45	30	3	0	1	7	398.35	467.40	1.0622
5c	7.60	85.27	32	6	0	1	8	403.80	433.50	0.4893
5d	7.64	39.45	29	3	0	1	7	380.46	388.51	0.9537
5e	7.65	48.68	31	4	0	1	8	406.01	418.53	0.86295
5f	7.70	48.68	31	4	0	1	8	406.01	418.53	0.8707

Note: Drug likeness of the synthesized compounds.
Abbreviations: MW, molecular weight; TPSA, topological polar surface area.
[a]Logarithm of partition coefficient between n-octanol and water (mi log *P*).
[b]Topological polar surface area (TPSA).
[c]Number of hydrogen bond acceptors (n-ON).
[d]Number of hydrogen bond donors (n-OHNH).
[e]Number of rotatable bonds (n-rotb).
[f]Molecular volume.
[g]Molecular weight.
[h]Blood brain barrier.

39.45–102.34 Å and is well below the limit of 160 Å, indicating good oral bioavailability. The upper limit for TPSA for a molecule to penetrate the brain is around 90 Å. The in silico predicted values (Fiser & Šali, 2003) point that compounds with log BB values more than 0.3 are considered to be highly absorbed through BBB whereas values between 0.3 and −0.1 and less than −0.1 are considered to be limited transported through BBB. All compounds of series **5a**-**5f** have log BB more than 0.3. On the contrary, compounds from series 3 and 4 presented log BB values between 0.3 and – 0.1 except for **3c** and **4c**, which have log BB values less than −0.1 and they are considered to be limited transported through BBB. Our findings do not support the permeability of them through BBB.

4 | CONCLUSIONS

In conclusion, 18 multi-substituted coumarins—six acetyloxy-derivatives, six hydroxy-derivatives, and six geranyloxy-derivatives—were synthesized, structurally characterized, and evaluated for their bioactivity. The results reveal that four coumarin analogues (**3a**, **3b**, **4d**, and **5c**) are strong antioxidant scavengers, while the 5-geranyloxy-compound **5f** is the best soybean lipoxygenase inhibitor. All the novel derivatives present allosteric interactions with the enzyme as it can be concluded from the modeling studies.

In regard to the cytotoxic activity, it was observed that among the three different types of substituents at position 5 of the coumarin core, the acetyloxy-group led to the most effective anticancer agents, especially for the compounds **3a** and **3b** bearing a bromo-substitution on the phenyl ring. The theoretical calculations for drug likeness of the derivatives showed that these molecules could be easily transported, diffused, and absorbed. Considering the calculated lipophilicity log *P* values, the most potent in cytotoxicity tests compounds **3a** and **3b** were found to be less than 5 and are in agreement with Lipinski's rule of five, suggesting satisfactory permeability across the cell membrane.

Overall, the presence of a bromo-substituent on the phenyl ring as well as of the acetyloxy moiety at position 5 on the coumarin core can be considered as key structural features for future design and development of new therapeutic anticancer and anti-inflammatory agents.

ACKNOWLEDGMENTS

E. K. gratefully acknowledges State Scholarships Foundation (IKY). This research is co-financed by Greece and the European Union (European Social Fund [ESF]) through the Operational Programme (Human Resources Development, Education and Lifelong Learning) in the context of the project "Scholarships Programme for post-graduate studies—2nd Study Cycle" (MIS-5003404), implemented by the State Scholarships Foundation (IKY).

A. K. gratefully acknowledges State Scholarships Foundation (IKY). This research is co-financed by Greece and the European Union (ESF) through the Operational Programme (Human Resources Development, Education and Lifelong Learning) in the context of the project "Strengthening Human Resources Research Potential via Doctorate Research" (MIS-5000432), implemented by the State Scholarships Foundation (IKY).

We are thankful to Biobyte and Dr. A. Leo for free use of C-QSAR and support.

We acknowledge support of this work by the project "An Open-Access Research Infrastructure of Chemical Biology and Target-Based Screening Technologies for Human and Animal Health, Agriculture and the Environment (OPENSCREEN-GR)" (MIS 5002691) which is implemented under the Action "Reinforcement of the Research and Innovation Infrastructure," funded by the Operational Programme "Competitiveness, Entrepreneurship and Innovation" (NSRF 2014-2020) and co-financed by Greece and the European Union (European Regional Development Fund).

CONFLICT OF INTEREST

There are no conflicts to declare.

ORCID

Anastasia Detsi https://orcid.org/0000-0001-8325-2980

REFERENCES

Akram, M. W., Fakhar-e-Alam, M., Atif, M., Butt, A. R., Asghar, A., Jamil, Y., … Wang, Z. M. (2018). In vitro evaluation of the toxic effects of MgO nanostructure in Hela cell line. *Scientific Reports*, *8*, 4576.

Alhassan, A., Abdullahi, M., Uba, A., & Umar, A. (2014). Prenylation of aromatic secondary metabolites: A new frontier for development of novel drugs. *Tropical Journal of Pharmaceutical Research*, *13*(2), 307.

Atta-ur-Rahman (2018). *Studies in natural products chemistry*. Amsterdam: Elsevier.

Bathula, C., Dangi, P., Hati, S., Agarwal, R., Munshi, P., Singh, A., … Sen, S. (2015). Diverse synthesis of natural product inspired fused and Spiro-heterocyclic scaffolds via ring distortion and ring construction strategies. *New Journal of Chemistry*, *39*, 9281–9292.

Berridge, M. V., & Tan, A. S. (1993). Characterization of the cellular reduction of 3-(4,5-Dimethylthiazol-2-Yl)-2,5-Diphenyltetrazolium bromide (MTT): Subcellular localization, substrate dependence, and involvement of mitochondrial electron transport in MTT reduction. *Archives of Biochemistry and Biophysics*, *303*(2), 474–482.

Bian, T., Vijendra, K. C., Wang, Y., Meacham, A., Hati, S., Cogle, C. R., … Xing, C. (2018). Exploring the structure–activity relationship and mechanism of a Chromene scaffold (CXL series) for its selective Antiproliferative activity toward multidrug-resistant cancer cells. *Journal of Medicinal Chemistry*, *61*(15), 6892–6903.

Biobyte Corp. C-QSAR Database. (n.d.). 201 West 4th Str., Suite 204, Claremont, CA 91711, USA.

Brash, A. R. (1999). Lipoxygenases: Occurrence, functions, catalysis, and acquisition of substrate. *The Journal of Biological Chemistry*, *274*, 23679–23682.

Burgess, A., Shah, K., Hough, O., & Hynynen, K. (2016). Vitro evaluation of 3-Arylcoumarin derivatives in A549 cell line. *Anticancer Research*, *15* (5), 477–491.

Crusz, S. M., & Balkwill, F. R. (2015). Inflammation and cancer: Advances and new agents. *Nature Reviews Clinical Oncology*, *12* (10), 584–596.

Curini, M., Epifano, F., Genovese, S., Menghini, L., Richi, D., Fraternale, D., … Bellachio, E. (2006). Lipoxygenase inhibitory activity of Boropinic acid, active principle of *Boronia Pinnata*. *Natural Product Communications*, *1*(12), 1141–1145.

Demir, S., Özen, C., Ünlüsoy, M. C., Öztürk, M., & Bozdağ-Dündar, O. (2019). Novel furochromone derivatives: Synthesis and anticancer activity studies. *Journal of Heterocyclic Chemistry*, *56*(4), 1341–1351.

Denisov, E. T., & Afanas'ev, I. B. (2005). *Oxidation and antioxidants in organic chemistry and biology*. Boca Raton: CRC Press: Taylor & Francis.

Detsi, A., Kontogiorgis, C., & Hadjipavlou-Litina, D. (2017). Coumarin derivatives: An updated patent review (2015-2016). *Expert Opinion on Therapeutic Patents*, *27*(11), 1201–1226.

Detsi, A., Majdalani, M., Kontogiorgis, C. A., Hadjipavlou-Litina, D., & Kefalas, P. (2009). Natural and synthetic 2′-Hydroxy-Chalcones and Aurones: Synthesis, characterization and evaluation of the antioxidant and soybean Lipoxygenase inhibitory activity. *Bioorganic & Medicinal Chemistry*, *17*(23), 8073–8085.

Dickens, W. A., Kuhn, G., Leng, M. J., Graham, A. G. C., Dowdeswell, J. A., Meredith, M. P., … Smith, J. A. (2019). Enhanced glacial discharge from the eastern Antarctic peninsula since the 1700s associated with a positive southern annular mode. *Scientific Reports*, *9*, 14606.

Dos Santos Nascimento, M. V., Arruda-Silva, F., Luz, A. B., Venzke, D., Queiroz, G. S., Mendes, B. G., … Dalmarco, E. M. (2015). 7-Prenyloxi-6-Methoxycoumarin from polygala Sabulosa A.W. Bennett regulates P38 MAPK and NF-KB pathways inhibiting the inflammation induced by carrageenan in the mouse model of pleurisy. *Inflammation & Allergy Drug Targets*, *14*(1), 37–46.

Fiorito, S., Epifano, F., Preziuso, F., Cacciatore, I., di Stefano, A., Taddeo, V. A., … Genovese, S. (2018). Natural oxyprenylated coumarins are modulators of melanogenesis. *European Journal of Medicinal Chemistry*, *152*, 274–282.

Fiorito, S., Epifano, F., Taddeo, V. A., & Genovese, S. (2018). Recent acquisitions on oxyprenylated secondary metabolites as anti-inflammatory agents. *European Journal of Medicinal Chemistry*, *153*, 116–122.

Fiser, A., & Šali, A. (2003). Modeller: Generation and refinement of homology-based protein structure models. *Methods in Enzymology*, *374*, 461–491.

Funk, C. D. (2001). Prostaglandins and leukotrienes: Advances in eicosanoid biology. *Science*, *294*, 1871–1875.

Garazd, Y., Garazd, M., & Lesyk, R. (2017). Synthesis and evaluation of anticancer activity of 6-pyrazolinylcoumarin derivatives. *Saudi Pharmaceutical Journal*, *25*(2), 214–223.

Genovese, S., Taddeo, V. A., Fiorito, S., Epifano, F., Marrelli, M., & Conforti, F. (2017). Inhibition of nitric oxide production by natural oxyprenylated coumarins and alkaloids in RAW 264.7 cells. *Phytochemistry Letters*, *20*, 181–185.

Goswami, S., Bhattacharya, D., Ghosh, C. K., Ghosh, B., Kaushik, S. D., Siruguri, V., & Krishna, P. S. R. (2018). Nonmonotonic particle-size-dependence of magnetoelectric coupling in strained nanosized particles of $BiFeO_3$. *Scientific Reports*, *8*, 3728.

Halgren, T. A. (1996). Merck molecular force field. I. Basis, form, scope, parameterization, and performance of MMFF94. *Journal of Computational Chemistry*, *17*(5–6), 490–519.

Hasan, M., Genovese, S., Fiorito, S., Epifano, F., & Witt-Enderby, P. A. (2017). Oxyprenylated Phenylpropanoids bind to MT1 melatonin receptors and inhibit breast cancer cell proliferation and migration. *Journal of Natural Products*, *80*(12), 3324–3329.

Hati, S., Tripathy, S., Dutta, P. K., Agarwal, R., Srinivasan, R., Singh, A., … Sen, S. (2016). Spiro[Pyrrolidine-3, 3′-Oxindole] as potent anti-breast cancer compounds: Their design, synthesis, biological evaluation and cellular target identification. *Scientific Reports*, *6*, 32213.

Hess, B., Kutzner, C., van der Spoel, D., & Lindahl, E. (2008). GROMACS 4: Algorithms for highly efficient, load-balanced, and scalable molecular simulation. *Journal of Chemical Theory and Computation*, *4*(3), 435–447.

Ibrar, A., Shehzadi, S. A., Saeed, F., & Khan, I. (2018). Developing hybrid molecule therapeutics for diverse enzyme inhibitory action: Active role of coumarin-based structural leads in drug discovery. *Bioorganic and Medicinal Chemistry*, *26*(13), 3731–3762.

Jabbari, A., Mousavian, M., Seyedi, S. M., Bakavoli, M., & Sadeghian, H. (2017). O-prenylated 3-carboxycoumarins as a novel class of 15-LOX-1 inhibitors. *PLoS One*, *12*(2), 1–21.

Justino, G. C., Rodrigues, M., Florêncio, M. H., & Mira, L. (2009). Structure and antioxidant activity of brominated flavonols and flavanones. *Journal of Mass Spectrometry*, *44*(10), 1459–1468.

Kavetsou, E., Gkionis, L., Galani, G., Gkolfinopoulou, C., Argyri, L., Pontiki, E., … Detsi, A. (2017). Synthesis of prenyloxy coumarin analogues and evaluation of their antioxidant, lipoxygenase (LOX) inhibitory and cytotoxic activity. *Medicinal Chemistry Research*, *26*(4), 856–866.

Lee, J. C., Shin, E. A., Kim, B., Kim, B. -I., Chitsazian-Yazdi, M., Iranshahi, M., & Kim, S.-H. (2017). Auraptene induces apoptosis via myeloid cell Leukemia 1-mediated activation of caspases in PC3 and DU145 prostate cancer cells. *Phytotherapy Research*, *31*(6), 891–898.

Lindorff-Larsen, K., Piana, S., Palmo, K., Maragakis, P., Klepeis, J. L., Dror, R. O., & Shaw, D. E. (2010). Improved side-chain torsion potentials for the Amber Ff99SB protein force field. *Proteins: Structure, Function, and Bioinformatics*, *78*(8), 1950–1958.

Lipinski, C. A., Lombardo, F., Dominy, B. W., & Feeney, P. J. (1997). Experimental and computational approaches to estimate solubility and permeability in drug discovery and development settings. *Advanced Drug Delivery Reviews*, *23*(1–3), 3–25.

Majumdar, P., Bathula, C., Basu, S. M., Das, S. K., Agarwal, R., Hati, S., … Das, B. B. (2015). Design, synthesis and evaluation of thiohydantoin derivatives as potent topoisomerase I (Top1) inhibitors with anticancer activity. *European Journal of Medicinal Chemistry*, *18*(102), 540–551.

Mansoori, B., Mohammadi, A., Davudian, S., Shirjang, S., & Baradaran, B. (2017). The different mechanisms of cancer drug resistance: A brief review. *Advanced Pharmaceutical Bulletin*, *7*(3), 339–348.

Matos, M. J., Vazquez-Rodriguez, S., Fonseca, A., Uriarte, E., Santana, L., & Borges, F. (2017). Heterocyclic antioxidants in nature: Coumarins. *Current Organic Chemistry*, *21*(4), 311–324.

Mazimba, O. (2017). Umbelliferone: Sources, chemistry and bioactivities review. *Bulletin of Faculty of Pharmacy, Cairo University*, *55*(2), 223–232.

Melagraki, G., Afantitis, A., Igglessi-Markopoulou, O., Detsi, A., Koufaki, M., Kontogiorgis, C., & Hadjipavlou-Litina, D. J. (2009). Synthesis and evaluation of the antioxidant and anti-inflammatory activity of novel Coumarin-3-aminoamides and their alpha-lipoic acid adducts. *European Journal of Medicinal Chemistry*, *44*(7), 3020–3026.

Musa, M. A., Latinwo, L. M., Joseph, M. Y., & Badisa, V. L. (2017). Identification of 7,8-diacetoxy-3-arylcoumarin derivative as a selective cytotoxic and apoptosis-inducing agent in a human prostate cancer cell line. *Anticancer Research*, *37*(11), 6005–6014.

Musa, M. A., Latinwo, L. M., Virgile, C., Badisa, V. L. D., & Gbadebo, A. J. (2015). Synthesis and in vitro evaluation of 3-(4-Nitrophenyl) Coumarin derivatives in tumor cell lines. *Bioorganic Chemistry*, *58*, 96–103.

O'Boyle, N. M., Banck, M., James, C. A., Morley, C., Vandermeersch, T., & Hutchison, G. R. (2011). Open babel: An open chemical toolbox. *Journal of Cheminformatics*, *3*(1), 33.

Okuyama, S., Minami, S., Shimada, N., Makihata, N., Nakajima, M., & Furukawa, Y. (2013). Anti-inflammatory and neuroprotective effects of auraptene, a citrus coumarin, following cerebral global ischemia in mice. *European Journal of Pharmacology*, *699*(1–3), 118–123.

Orafaie, A., Matin, M. M., & Sadeghian, H. (2018). The importance of 15-lipoxygenase inhibitors in cancer treatment. *Cancer and Metastasis Reviews*, *37*, 397–408.

Park, D., Son, K., Hwang, Y., Ko, J., Lee, Y., Doh, J., & Jeon, N. L. (2019). High-throughput microfluidic 3D cytotoxicity assay for cancer immunotherapy (CACI-IMPACT platform). *Frontiers in Immunology*, *10*, 1133.

Pettersen, E. F., Goddard, T. D., Huang, C. C., Couch, G. S., Greenblatt, D. M., Meng, E. C., & Ferrin, T. E. (2004). UCSF chimera-a visualization system for exploratory research and analysis. *Journal of Computational Chemistry*, *25*(13), 1605–1612.

Pontiki, E., & Hadjipavlou-Litina, D. (2008). Lipoxygenase inhibitors: A comparative QSAR study review and evaluation of new QSARs. *Medicinal Research Reviews*, *28*(1), 39–117.

Qi, K., Li, Y., Huang, K., Xiong, X., Feng, C., Zhang, C., & Weng, W. (2019). Pre-application of arsenic trioxide may potentiate cytotoxic effects of vinorelbine/docetaxel on neuroblastoma SK-N-SH cells. *Biomedicine & Pharmacotherapy*, *113*, 108665.

Raj, H. G., Kohli, E., Rohil, V., Dwarakanath, B. S., Parmar, V. S., Malik, S., … Olsen, C. E. (2001). Acetoxy-4-Methylcoumarins confer differential protection from aflatoxin B1-induced micronuclei and apoptosis in lung and bone marrow cells. *Mutation Research—Genetic Toxicology and Environmental Mutagenesis*, *494*(1–2), 31–40.

Ricci, F., Carrassa, L., Christodoulou, M. S., Passarella, D., Michel, B., Benhida, R., … Damia, G. (2018). A high-throughput screening of a chemical compound library in ovarian cancer stem cells. *Combinatorial Chemistry & High Throughput Screening*, *21*(1), 50–56.

Roussaki, M., Kontogiorgis, C. A., Hadjipavlou-Litina, D., Hamilakis, S., & Detsi, A. (2010). A novel synthesis of 3-aryl coumarins and evaluation of their antioxidant and Lipoxygenase inhibitory activity. *Bioorganic & Medicinal Chemistry Letters*, *20*(13), 3889–3892.

Roussaki, M., Zelianaios, K., Kavetsou, E., Hamilakis, S., Hadjipavlou-Litina, D., Kontogiorgis, C., … Detsi, A. (2014). Structural modifications of Coumarin derivatives: Determination of antioxidant and lipoxygenase (LOX) inhibitory activity. *Bioorganic & Medicinal Chemistry*, *22*(23), 6586–6594.

Schneider, C., & Pozzi, A. (2011). Cyclooxygenases and lipoxygenases in cancer. *Cancer and Metastasis Reviews*, *30*(3–4), 277–294.

Senapati, S., Mahanta, A. K., Kumar, S., & Maiti, P. (2018). Controlled drug delivery vehicles for cancer treatment and their performance. *Signal Transduction and Targeted Therapy*, *3*(1), 7.

Seshadri, V. (1952). Proceedings-Indian Academy of Sciences, Section A, 75, 80(5).

Simijonović, D., Vlachou, E. -E., Petrović, Z. D., Hadjipavlou-Litina, D. J., Litinas, κ. E., Stanković, N., … Mladenović, M. P. (2018). Dicoumarol derivatives: Green synthesis and molecular modelling studies of their anti-LOX activity. *Bioorganic Chemistry*, *80*, 741–752.

Sousa da Silva, A. W., & Vranken, W. F. (2012). ACPYPE - AnteChamber PYthon Parser InterfacE. *BMC Research Notes*, *5*(1), 367.

Swift, L., Zhang, C., Trippett, T., & Narendran, A. (2019). Potent in vitro and xenograft antitumor activity of a novel agent, PV-10, against relapsed and refractory neuroblastoma. *OncoTargets and Therapy*, *18*(12), 1293–1307.

Thakur, A., Singla, R., & Jaitak, V. (2015). Coumarins as anticancer agents: A review on synthetic strategies, mechanism of action and SAR studies. *European Journal of Medicinal Chemistry*, *101*, 476–495.

Trott, O., & Olson, A. J. (2010). AutoDock Vina: Improving the speed and accuracy of docking with a new scoring function, efficient optimization, and Multithreading. *Journal of computational chemistry*, *31*(2), 455–461.

Wang, J., Wang, W., Kollman, P. A., & Case, D. A. (2006). Automatic atom type and bond type perception in molecular mechanical calculations. *Journal of Molecular Graphics and Modelling*, *25*(2), 247–260.

Wiart, C. (2013). *Lead compounds from medicinal plants for the treatment of cancer*. London: Elsevier Academic Press.

Yang, X., Li, S., Li, W., Chen, J., Xiao, X., Wang, Y., … Chen, L. (2013). Inactivation of Lysyl oxidase by β-aminopropionitrile inhibits hypoxia-induced invasion and migration of cervical cancer cells. *Oncology Reports*, *29*(2), 541–548.

Yen, C. M., Tsai, C. W., Chang, W. S., Yang, Y. C., Hung, Y. W., Lee, H. T., … Bau, D. T. (2018). Novel combination of arsenic trioxide (As2O3) plus resveratrol in inducing programmed cell death of human neuroblastoma SK-N-SH cells. *Cancer Genomics Proteomics*, *15*(6), 453–460.

How to cite this article: Kavetsou E, Katopodi A, Argyri L, et al. Novel 3-aryl-5-substituted-coumarin analogues: Synthesis and bioactivity profile. *Drug Dev Res*. 2020;1–14. https://doi.org/10.1002/ddr.21639